Design and synthesis of haem-binding peptides. Relationship between haem-binding properties and catalytic activities

Seiji Sakamoto, Akihiko Ueno and Hisakazu Mihara *

Department of Bioengineering, Faculty of Bioscience and Biotechnology, Tokyo Institute of Technology, Midori-ku, Yokohama 226-8501, Japan

Received (in Cambridge) 21st July 1998, Accepted 3rd September 1998

We have designed and synthesized two series of amphiphilic two-α-helix peptides, that bound Fe^{III}–mesoporphyrin (haem) through a ligation of two His residues. The interaction between the peptides and the haem was characterized by UV–VIS and circular dichroism (CD) measurements. The first series of peptides, designed on the basis of the coiled-coil motif, showed a unique haem binding property which was dependent on the concentration of trifluoroethanol (TFE) present. The peptides bound the haem effectively only when the two-α-helix structures were controlled by the addition of 10–25% TFE. These results indicated that the haem binding ability of the peptides could be regulated by the change in peptide conformation with TFE. The second series of two-α-helix peptides, designed on the basis of the amphiphilic α-helix motif, but not of the coiled-coil motif, formed an α-helix structure and bound the haem in a buffer. Furthermore, in the presence of peptides, the haem showed strong induced CD peaks at the Soret region, implying that the haem chromophore was highly oriented in the peptide structures. The catalytic activity of the haem bound to the peptides, which was similar to that of peroxidase, was significantly depressed with increased binding constants and the Soret-CD intensities. It was demonstrated that the catalytic activity of the haem was correlated with the rigidity and orientation of the *b*-type haem in the polypeptides.

Introduction

A variety of haemproteins display diverse functions in nature, such as oxygen carrier/storage, electron transfer, redox catalysis[1,2] and transmission of information,[3] though they employ a simple iron porphyrin as a common cofactor. Each specific function of haemproteins is regulated by environments around a haem formed by polypeptides, including axial ligands, arrangements of amino acids and polypeptide three-dimensional (3D) structures.[4] Over the years, in order to elucidate the control mechanisms of haemprotein functions, many studies using small porphyrin model compounds and mutated proteins have been carried out. Small model porphyrin compounds have been useful tools in proposing the reaction mechanisms of haemproteins.[5–8] However, they cannot reproduce special environments provided by polypeptides, which are essential for the specific recognition and reaction of natural haemproteins. Site-directed mutagenesis has been also a basic method for the study of the structure–function relationships of natural proteins. It is not easy, however, to understand the detailed mechanisms of diverse haemprotein functions, due to the large size and structural complexity of the natural proteins. Thus, it is necessary to establish a structural model system which has more native-like properties and which can remove the complexity of the natural counterpart.

Considerable effort has also been devoted to the construction of *de novo* designed polypeptide 3D structures[9–18] and to the conjugation of porphyrin molecules *via* chelation[19–23] or covalent linkages[24–28] with peptides. For example, Dutton, DeGrado and co-workers have succeeded in the design and synthesis of artificial polypeptides which have Fe–protoporphyrin IX and other functional chromophores in four-α-helix bundle structures as models of electron transfer proteins.[19] As an example of a covalently attached haem–peptide, Pavone *et al.* recently reported the circular dichroism (CD) and NMR characterization of a designed helix–haem–helix structure.[27] Because these artificial haem-conjugated peptides are characterized as having a well defined 3D structure with relatively simple amino acid compositions, they will be a powerful tool in studying the structural roles of polypeptides in the function of proteins. In the present study, to develop a mini-haemprotein that meets the minimal requirements for the function, we have synthesized two series of originally designed polypeptides which were composed of two α-helices and which could bind the haem (Fig. 1 and 2). The first series of peptides were designed to find the conformational requirements for effective haem-binding. By using these peptides, we examined the difference in haem-binding ability with the conformational changes of the peptides in trifluoroethanol (TFE)–buffer solutions. Next, we have constructed stable haem–peptide conjugates in a buffer, on the basis of the results obtained from the first series of peptides. Furthermore, the catalytic activity of the haem–peptide conjugates, which resembled that of peroxidase, was examined, in order to know how the haem activity was regulated by the polypeptide binding.

Results

Design and synthesis

For frameworks of the peptides capable of binding a haem, we used structures with two α-helices (2α-helix), because of their relatively simple 3D structure.[14] At the first stage, in order to evaluate haem binding properties depending on the peptide length, we designed three peptides, H2α(14), H2α(17) and H2α(21), which have different chain lengths and different numbers of Leu residues. The 14-, 17- and 21-peptide segments were constructed from amino acid sequences of coiled-coil proteins,[29] which have heptad repeats $(abcdefg)_n$ with hydrophobic residues, such as Leu, at the *a* and *d* positions. Each peptide segment consists of repeats of the heptad sequence where the *a* and *d* residues are Leu, *f* is hydrophilic Gln, *b* and *c* are Ala, *e* is Glu and *g* is Lys. To construct a structure consisting of two parallel α-helices, the two segments were dimerized by the disulfide linkage of Cys residues at the C-terminals with a flexible spacer of β-Ala. As axial ligands of haem, His residues

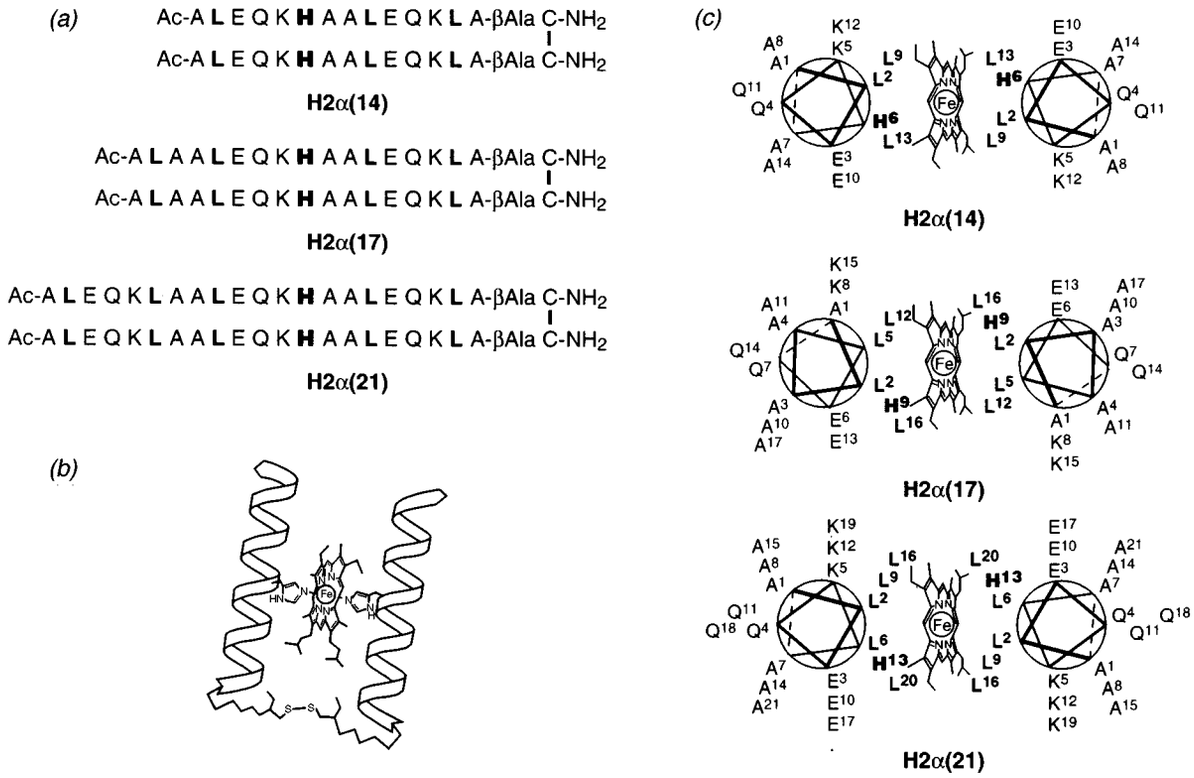

Fig. 1 Structure of the first series of peptides designed on the basis of coiled-coil motif. (*a*) Amino acid sequence of the H2α(14), H2α(17) and H2α(21). (*b*) Illustration of the 2α-helix peptide structure bound to the haem. (*c*) Helix wheel drawings of the 14-, 17- and 21-peptides in coiled-coil form.

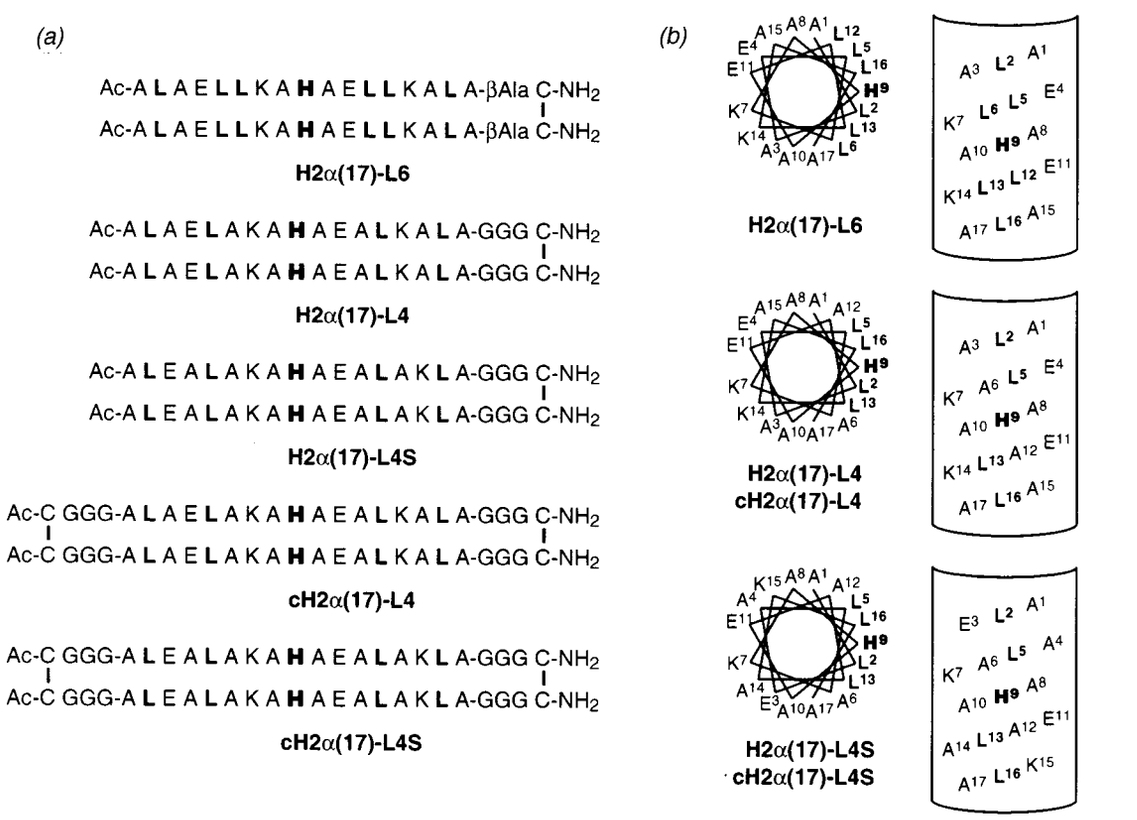

Fig. 2 Designed structure of the second series of peptides. (*a*) Amino acid sequence of the H2α(17)-L6, H2α(17)-L4, H2α(17)-L4S, cH2α(17)-L4 and cH2α(17)-L4S. (*b*) Illustration of helix wheel and net drawings of the 17-peptides.

were introduced at the 6th, 9th and 14th position in each peptide instead of Leu to coordinate a haem inside a hydrophobic pocket between two α-helices. In the designed structure, a haem would be deployed parallel to the helix.

The second series of peptides, H2α(17)-L6, H2α(17)-L4, H2α(17)-L4S, were also designed to form a parallel 2α-helix structure by the linkage of Cys residues. The 17-segments in the peptides were designed to take an amphiphilic α-helix structure (Fig. 2), although the arrangements of hydrophobic Leu residues were not ordered by the heptad rule like the coiled-coil

motif. As axial ligands of haem, His residues were also deployed at the 9th position to coordinate a haem inside a hydrophobic pocket between two α-helices. In the new designed structure, His[9] was positioned at the center of the hydrophobic region on the amphiphilic α-helix as shown by the wheel and net drawings of the 17-segments (Fig. 2). The 17-segment in H2α(17)-L6 was initially designed, in which 6 Leu residues were deployed on the hydrophobic face of the amphiphilic α-helix.

In order to evaluate the haem binding property due to the hydrophobicity of the sequence, the related 17-segment in H2α(17)-L4 was designed on the basis of H2α(17)-L6 to reduce the hydrophobicity of the peptide using two Ala residues instead of Leu residues at the 5th and 12th positions. In the case of H2α(17)-L4, the structure of a spacer β-Ala was replaced by a more flexible and longer spacer -Gly-Gly-Gly-. The peptide H2α(17)-L4S was designed on the basis of H2α(17)-L4 to stabilize the α-helix structure with intrahelix (i, $i + 4$) salt bridges[30] by replacing Ala[3], Glu[4], Lys[14] and Ala[15] in the L4 segment with Glu[3], Ala[4], Ala[14] and Lys[15] in the L4S segment. As a result of these replacements, H2α(17)-L4S would possess two (i, $i + 4$) Glu-Lys ion pairs at the (3, 7) and (11, 15) positions. Additionally, to attain further structural stabilization of the peptides, we designed two cyclic peptides, cH2α(17)-L4 and cH2α(17)-L4S. The peptides, cH2α(17)-L4 and cH2α(17)-L4S had the same 17-peptide segments as H2α(17)-L4 and H2α(17)-L4S, respectively. In addition, the peptides had the second disulfide linkage[31] at the N-terminal with a flexible spacer of -Gly-Gly-Gly-.

All the peptides were synthesized by the solid-phase method using the Fmoc-strategy (Fmoc, fluoren-9-ylmethoxycarbonyl).[32] The disulfide bond at the C-terminals was formed by air-oxidation to give the parallel 2α-helix structure. The cyclic peptides, cH2α(17)-L4 and cH2α(17)-L4S were synthesized in a manner similar to that described above. However, in order to form specific intramolecular cross-linkages, selectively cleavable sulfhydryl protecting groups were employed [Cys at the N-terminal was protected with the acetamidomethyl (Acm) group and Cys at the C-terminal was protected with the trityl (Trt) group]. Formation of the second cross-linkage was simultaneously achieved with detachment of two Acm groups at the N-terminals by treatment using trichloromethylsilane in the presence of diphenyl sulfoxide in TFA.[33] All peptides were purified with HPLC to high purity (>98% on HPLC). The peptides and intermediates were identified by amino acid analysis and matrix assisted laser desorption ionization time-of-flight mass spectrometry (MALDI-TOFMS).

Far-UV CD Study of H2α(14), H2α(17) and H2α(21)

CD spectra of H2α(14), H2α(17) and H2α(21) in 2.0×10^{-2} mol dm^{-3} Tris HCl buffer, pH 7.4, containing various amounts of TFE, were examined. CD studies of H2α(14) in the TFE–buffer solutions were reported in the previous communication.[23a] CD spectra of H2α(17) showed a dependence on the TFE concentration similar to that of H2α(14). In the buffer, the conformations of H2α(14) and H2α(17) were almost random due to the introduction of His residues, having a helix-breaking nature[34] (Fig. 3). The α-helicity of the peptide was estimated from the ellipticity at 222 nm.[35] With an increasing percentage volume of TFE, which is known to be an α-helix stabilizing solvent,[29a] the α-helicities of H2α(14) and H2α(17) were gradually increased (Fig. 3). In the presence of haem (1.0 equiv.), a further increase in the α-helicity of both peptides was obtained at 10–20% TFE (Fig. 3, closed circles). The largest increase of the α-helicity of H2α(14) and H2α(17) by the addition of haem was obtained at around 15% and 10% TFE, respectively.

To confirm that the improvement in α-helicity was due to the haem binding by the His residues in the 2α-helix peptides, 1-methylimidazole was added to inhibit coordination of the haem with the peptide. With increasing concentration of the exogenous ligand, the α-helicity of H2α(14) was decreased to 40%, which coincided with the value of H2α(14) in the absence of the haem [Fig. 4(*a*)]. Furthermore, the increase in α-helicity was sensitive to the solution pH. No increase of α-helicity was observed by the addition of haem at acidic pH (2.0–6.0) [Fig. 4(*b*)]. The midpoint of α-helix improvement was approximately pH 6.6. Because the pK_a of His in a random peptide is about 6.4,[36] the pH effect is attributed to the protonation of His side chains such that they cannot act as a ligand. Broo *et al.* reported that the pK_a of the His residue in the folded peptide was changed by the environment around the His residue.[17b,c] In our case, however, the pK_a of the His residue seemed not to be significantly affected by the residues in the vicinity of the His upon folding or by the presence of 15% TFE. Therefore, we conclude that the increase in α-helicity of H2α(14) and H2α(17) took place *via* haem binding by ligation with the His residues. The haem binding of H2α(14) and H2α(17) was regulated by the helix annealing with an appropriate amount of TFE.

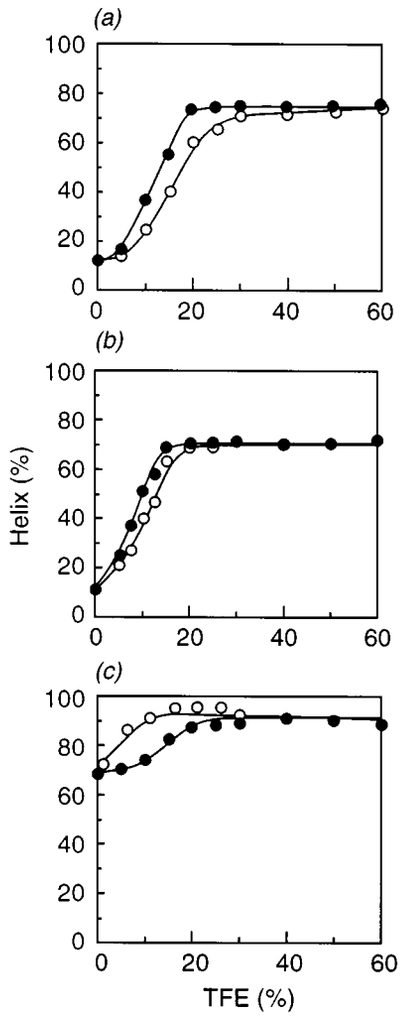

Fig. 3 Effect of TFE content on the α-helicity of (*a*) H2α(14), (*b*) H2α(17) and (*c*) H2α(21) in the absence (○) and presence of haem (2.0×10^{-5} mol dm^{-3}, 1.0 equiv.) (●) in 2.0×10^{-2} mol dm^{-3} Tris HCl buffer, pH 7.4 at 25 °C [peptide] = 2.0×10^{-5} mol dm^{-3}. The α-helicity (%) was estimated by the equation of Scholtz *et al.*[35]

In contrast to the two peptides, H2α(21) took an α-helical structure in the buffer. Because H2α(21) was the longest peptide among three and had five Leu residues in a segment, introduction of hydrophilic His residues did not significantly affect the hydrophobic interaction between the amphiphilic α-helix segments. H2α(21) did not bind the haem in the buffer, although it was α-helical. As for H2α(14) and H2α(17), TFE addition assisted the haem binding. With an increasing percentage

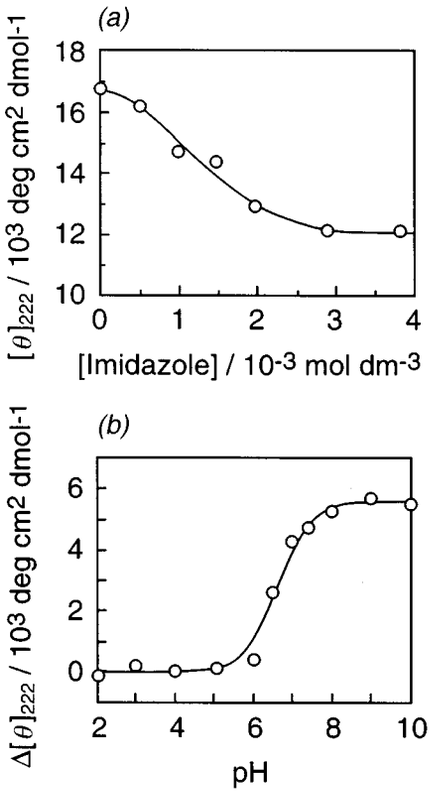

Fig. 4 (*a*) Ellipticity change at 222 nm of H2α(14) with 1.0 equiv. of haem with increasing 1-methylimidazole concentration in the buffer containing 15% TFE at 25 °C. (*b*) α-Helix improvement of H2α(14) by the addition of the haem (1.0 equiv.) in 15% TFE at pH ranging from 2.0 to 10.0 at 25 °C. Data are fitted by an equation for pH titration. [peptide] = 2.0×10^{-5} mol dm^{-3}.

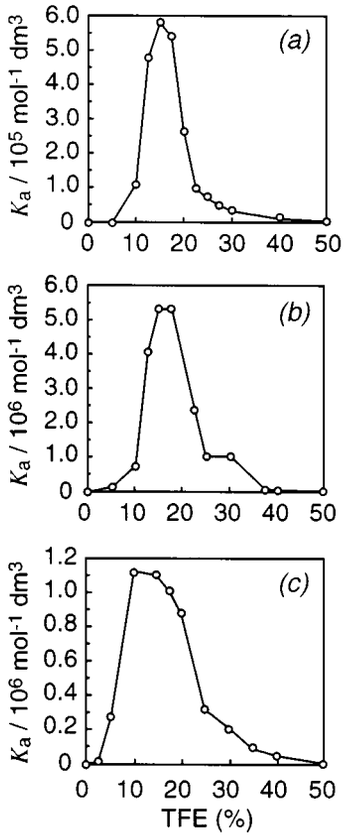

Fig. 5 Effect of TFE content on the binding constant for (*a*) H2α(14), (*b*) H2α(17) and (*c*) H2α(21) with the haem.

volume of TFE, the α-helicity of H2α(21) with the haem was slightly increased [Fig. 3(*c*)]. However, the increase of the α-helicity of H2α(21) was lower than that without the haem in the 10–20% TFE range. Presumably, insertion of a bulky haem group into the hydrophobic pocket in the H2α(21) might perturb the coiled-coil packing and destabilize the α-helix structure. The largest decrease of α-helicity of H2α(21) with the addition of haem also occurred at around 10% TFE. The haem binding of H2α(21) was attained by the loss of the helix packing with an appropriate amount of TFE.

UV–VIS spectra of haem with H2α(14), H2α(17) and H2α(21)

UV–VIS titration of the haem with H2α(14), H2α(17) and H2α(21) was carried out in buffer containing various amounts of TFE. The results for H2α(14) were reported in the previous communication.[23a] As for H2α(14), H2α(17) and H2α(21) showed the unique haem-binding property which was dependent on the concentration of TFE. As shown in the CD studies, the binding constants for the haem with the peptides, determined from the absorbance change at the Soret band (401 nm) using a single site binding equation,[37] were strongly dependent on the concentration of TFE (Fig. 5). The three peptides showed the highest binding constants at around 15% TFE [K_a: H2α(14), 5.8×10^5 mol^{-1} dm^3; H2α(17), 5.3×10^6 mol^{-1} dm^3; H2α(21), 1.1×10^6 mol^{-1} dm^3]. Among the peptides, H2α(17) was the strongest haem-binder. UV–VIS spectra of the haem bound to the peptides in 15% TFE indicated that the iron(III) was predominantly low-spin, consistent with bis-His coordination.[38] Spectral features included the sharp Soret band at 401 nm and a broad α/β band near 530 nm.

In contrast, the peptides could not bind the haem effectively at <10% and >25% TFE. These TFE titrations revealed that the 2α-helix structure and the consequent formation of a hydrophobic pocket were important for the haem-binding. In the cases of H2α(14) and H2α(17), because the conformation of the peptides is predominantly random at lower TFE concentrations (<10%), the hydrophobic pocket for the haem-binding is not formed. On the other hand, at higher TFE concentrations (>25%), the 2α-helix structure is destroyed so that each α-helix segment is free to move.[14a] Additionally, it is expected that hydrophobic interactions between the peptide and haem are also weakened at higher TFE concentrations. Because there is no hydrophobic pocket at either lower or higher TFE concentration, the peptides cannot bind the haem effectively. The monomer peptide H1α(14) and 1-methylimidazole needed a concentration of *ca.* 10^{-3} mol dm^{-3} for the haem-binding and did not show such TFE dependencies. These results also confirm that the formation of the 2α-helix structure is essential for haem-binding at the ~10^{-6} mol dm^{-3} level. In the case of H2α(21), which took a 70% α-helix structure in the buffer, tight helix–helix packing of the 2α-helix structure at the lower TFE concentration (<10%) seemed to inhibit the insertion of haem into the hydrophobic pocket. With the addition of 10–20% TFE, H2α(21) could bind the haem effectively, because the hydrophobic interaction between the helices was reduced. Although the excess amounts of TFE (>25%) inhibited the haem binding due to the disruption of the 2α-helix structure and/or the weakened hydrophobic interaction between the haem and the peptide, an appropriate amount of TFE (10–20%) could assist the haem binding. These results indicated that the haem binding ability of the peptides was controlled by the peptide conformation with TFE. This characteristic feature of the peptides seemed to be due to the His orientation in the 2α-helix structures constructed by the coiled-coil motif [Fig. 1(*c*)].

Far-UV CD study and thermal denaturation of H2α(17)-L6, H2α(17)-L4, H2α(17)-L4S, cH2α(17)-L4 and cH2α(17)-L4S

In order to construct a haem–peptide conjugate in an aqueous solution, the second series of 2α-helix peptides were designed

Table 1 α-Helix contents[a] and midpoints of thermal transition (T_m)[b] of the peptides in the absence and presence of haem

Peptide	α-Helix content (%)		T_m/°C		
	Without Haem	With Haem	Without Haem	With Haem	ΔT_m/°C
H2α(17)-L6	69	70	n. d.[c]	n. d.[c]	n. d.[c]
H2α(17)-L4	46	61	35	58	23
cH2α(17)-L4	62	74	46	70	24
H2α(17)-L4S	67	75	42	63	21
cH2α(17)-L4S	89	90	n. d.[c]	n. d.[c]	n. d.[c]

[a] α-Helix contents were estimated from the molecular ellipticity at 222 nm according to the equation of J. M. Scholtz *et al.* [ref. 35], [peptide] = 1.0×10^{-5} mol dm^{-3}; [haem] = 1.0×10^{-5} mol dm^{-3}, 25 °C. [b] T_m of peptides was taken as the temperature at which half of the peptide was unfolded. [c] Not determined.

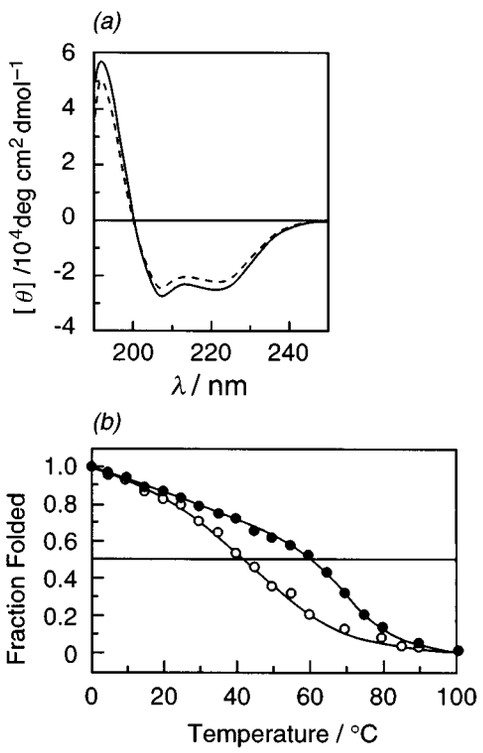

Fig. 6 (*a*) CD spectra of peptide, H2α(17)-L4S in the absence (– – –) and presence (——) of haem (1.0 equiv.) in the buffer, pH 7.4, at 25 °C. [peptide] = 1.0×10^{-5} mol dm^{-3}. (*b*) Temperature denaturation profiles of H2α(17)-L4S in the absence (○) and presence of haem (1.0×10^{-5} mol dm^{-3}, 1.0 equiv.) (●) in the buffer, pH 7.4. [peptide] = 1.0×10^{-5} mol dm^{-3}.

based on the amphiphilic α-helix motif. In the buffer, all the peptides showed a typical α-helical CD pattern with double negative maxima both in the absence and presence of haem [Fig. 6(*a*)]. The α-helical contents[35] of these peptides are summarized in Table 1. The α-helicity of H2α(17)-L4 was decreased compared with the original peptide H2α(17)-L6. The replacement of two Leu to Ala residues might decrease the hydrophobic interaction stabilizing the 2α-helix structure. Although the substitution decreased the α-helicity, this decrease might be reversed by the introduction of intrahelix electrostatic interactions[30] or cyclization of the 2α-helix structure by the second disulfide linkage.[31] The peptide H2α(17)-L4S was designed based on H2α(17)-L4, to form the intrahelix (*i*, *i* + 4) salt bridges by changing the position of Glu, Lys and Ala. Additionally, the peptides cH2α(17)-L4 and cH2α(17)-L4S have the second disulfide linkage at the N-terminals. Indeed, the α-helicity of H2α(17)-L4S and cH2α(17)-L4 was increased by a factor of 1.5 and 1.3, respectively, compared with that of H2α(17)-L4. Furthermore, the cyclic peptide cH2α(17)-L4S, which bore both α-helix stabilizing factors, took an almost complete α-helical structure (89%), 1.9 times higher than H2α(17)-L4. Interestingly, the helical contents of the peptides, except for H2α(17)-L6 and cH2α(17)-L4S, increased significantly with the addition of haem, similarly to H2α(14) and H2α(17). These results demonstrated the importance of the haem cofactor for the peptide folding.

The thermal stability of the second series of peptides in the absence and presence of haem was examined by CD measurements [Fig. 6(*b*) and Table 1]. Unfortunately, both in the absence and presence of haem, the peptides H2α(17)-L6 and cH2α(17)-L4S were so stable that they were not completely denatured in the temperature range. However, the other peptides exhibited a cooperative thermal denaturation in the absence of haem. The CD spectra of these peptides at various temperatures had an isodichroic point at around 203–205 nm, suggesting that denaturations occurred in a cooperative two-state process. The midpoint of thermal transition (T_m) for cH2α(17)-L4 and H2α(17)-L4S (46 °C and 42 °C, respectively) were larger than that of H2α(17)-L4 (35 °C) (Table 1), which had a lower α-helicity than the other peptides. As shown in Fig. 6(*b*) and Table 1, the haem binding remarkably increased the T_m value of the three peptides by 21–24 °C. These results indicated that the haem binding enhanced the stability of the 2α-helix structure, as well as the α-helicity. Similar conformational stabilization of the peptides by the introduction of a cofactor has been reported in the case of some artificial haem-conjugated polypeptides[19a,20–23] and natural haemproteins, such as myoglobin,[39] cytochrome *c*,[40] cytochrome b_5[41] and cytochrome b_{562}.[42] The peptides and proteins were almost fully folded and stabilized by the haem-binding *via* the formation of a metal–ligand bond and/or the hydrophobic interaction between haem and the helical segments.

UV–VIS spectra of haem with H2α(17)-L6, H2α(17)-L4, H2α(17)-L4S, cH2α(17)-L4 and cH2α(17)-L4S

UV–VIS titration of the haem with the second series of peptides was carried out in the buffer and 15% TFE solution, respectively. As an example, the result for H2α(17)-L4S in buffer is shown in Fig. 7(*a*). In the buffer, with increasing concentration of H2α(17)-L4S, an increase of the Soret band at 405 nm and α/β band near 530 nm, and a decrease of the band around 355 nm were observed. That is, with the addition of the peptide, the Fe^{III} in haem was converted from the high-spin to predominantly the low-spin form, with an isosbestic point at 390 nm.[38] These spectral features of the haem in the presence of H2α(17)-L4S were almost the same as those of haem bound to the first series of peptides. On the addition of other peptides to the haem, similar results were observed (Table 2). These results indicated that the peptides could bind the haem in the buffer *via* the ligation of two His residues.

The plots of absorbance change in the Soret band as a function of peptide concentration showed the bending point to be at the 1/1 [peptide]/[haem] ratio, suggesting that the peptides bind the haem with 1/1 stoichiometry. The binding constants determined from the absorbance change at the Soret band using a single site binding equation,[37] were in the order of 10^6–10^7 mol^{-1} dm^3 (Table 2). The cyclic peptide cH2α(17)-L4S showed the highest affinity for the haem ($K_a = 1.0 \times 10^7$ mol^{-1} dm^3). The most hydrophobic H2α(17)-L6 showed the lowest binding constant ($K_a = 5.6 \times 10^6$ mol^{-1} dm^3) among the peptides, suggesting that the tight helix–helix packing of the 2α-helix structure prevented the smooth insertion of haem into the hydrophobic pocket, as in the case of H2α(21). This suggestion was also confirmed by the titration experiments in 15% TFE solution, in which H2α(17)-L6 showed a binding constant ($K_a = 3.0 \times 10^7$ mol^{-1} dm^3) comparable to that of the other peptides ($K_a = 1.4$–3.5×10^7 mol^{-1} dm^3) (Table 2). The addition of

Table 2 UV–VIS spectral data of the haem bound to the peptides and binding constants (K_a)[a] of the peptides with the haem in the buffer and 15% TFE solution

	UV–VIS Soret, λ_{max}/nm		UV–VIS α/β, λ_{max}/nm		K_a/mol^{-1} dm^3	
Peptide	Ferric	Ferrous[b]	Ferric	Ferrous[b]	Buffer	15% TFE
H2α(17)-L6	403	413	526	546/519	5.6×10^6	3.0×10^7
H2α(17)-L4	404	413	529	550/521	7.3×10^6	3.5×10^7
cH2α(17)-L4	404	413	528	549/520	7.3×10^6	1.4×10^7
H2α(17)-L4S	405	413	527	550/520	8.3×10^6	1.7×10^7
cH2α(17)-L4S	405	413	526	550/520	1.0×10^7	1.3×10^7

[a] Binding constants were estimated from absorbance changes at the Soret band using a single site binding equation, [haem] = 1.0×10^{-5} mol dm^{-3}, 25 °C. [b] Iron(III) of the haem bound to the peptides was reduced with dithionite.

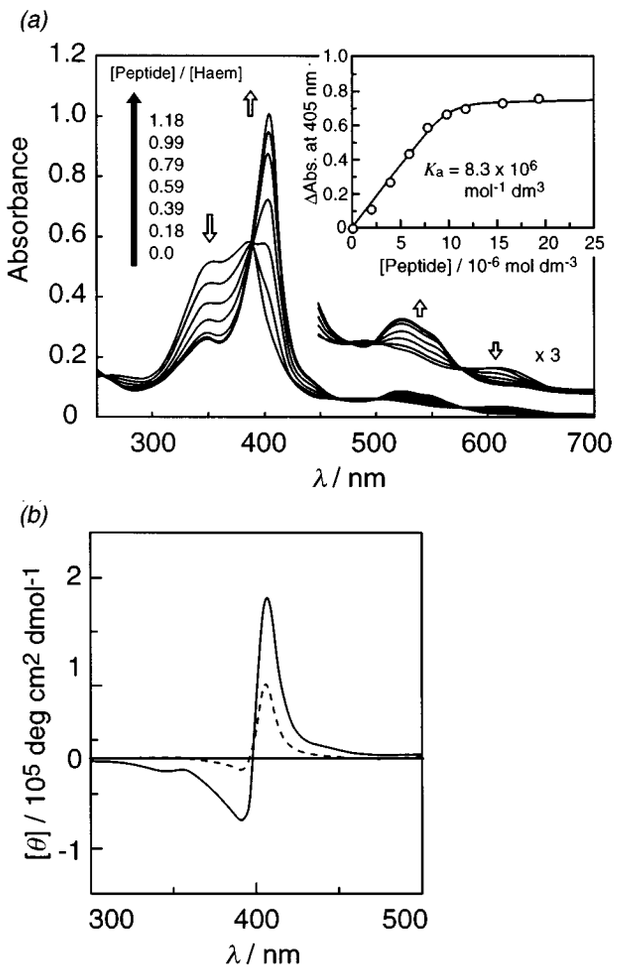

Fig. 7 (*a*) UV–VIS spectra of the haem with increasing H2α(17)-L4S concentration in the buffer at 25 °C. [haem] = 1.0×10^{-5} mol dm^{-3}. (*b*) CD spectra of haem at the Soret region in the presence of H2α(17)-L4S in the buffer (——) and 15% TFE–buffer solution (– – –) at 25 °C. [haem] = 1.0×10^{-5} mol dm^{-3}, [peptide] = 1.2×10^{-5} mol dm^{-3}.

15% TFE would loosen the tight packing of helices, resulting in the increase of binding constant.

CD spectra of haem bound to the peptides

The CD features of haem bound to the peptides were investigated in the Soret band region (300–500 nm) in the buffer and the 15% TFE–buffer solution. In the buffer, with the addition of peptides H2α(17)-L6, H2α(17)-L4, H2α(17)-L4S, cH2α(17)-L4 and cH2α(17)-L4S (1.2 equiv.), the haem showed induced CD peaks, which were characterized by a strong positive peak at around 405–410 nm ($[\theta]_{max} = 7.8$–21.8×10^5 deg cm^2 dmol^{-1}) and a negative peak at around 390 nm ($[\theta]_{max} = -1.0$ to -9.7×10^4 deg cm^2 dmol^{-1}) [Fig. 7(*b*)]. Since the haem group is a symmetrical chromophore, the haem itself should exhibit no inherent optical activity. Thus, the obtained CD feature confirmed that the haem was chirally localized and oriented in the 2α-helix peptides.

So far, Cotton effects arising from haem have been studied in a number of haemproteins and some haem-conjugated peptides.[23b,27,28,38] A great variety in the signs, magnitudes and shapes of the CD curves have been observed for the haem-transitions in these proteins and peptides, depending on the protein environments around the haem and the oxidation and coordination states of the central iron. The haem Soret band has been characterized essentially as a π–π* transition of porphyrin, two nearly degenerate electronic transitions (B_x and B_y) which are polarized perpendicular to each other and which are of opposite signs.[38] Various possible mechanisms have been proposed for the origin of the Soret–Cotton effect. For example, Hsu and Woody have shown that the shape of the Soret-CD band depends on the direction of polarization of the B_x and B_y components in the haem framework.[43] Additionally, Mizutani *et al.* reported that the complexes between zinc porphyrin and amino acid esters exhibited split type induced CD in the Soret region.[44] They have argued that the coupling interactions between porphyrin and the carbonyl group are important contributors to the Soret–Cotton effect in their model systems and that the relative geometries of the porphyrin plane and the carbonyl group determine the shape of the Soret-CD curves. The obtained Soret-CD band in our peptide–haem conjugates might be caused by a coupling interaction of π–π* haem transitions with π–π* and n–π* transitions localized in the polypeptide backbone. In other haem–peptide conjugates reported independently by Pavone *et al.*[27] or Benson *et al.*,[28] it was also indicated that the interaction between the Soret transition dipoles and the peptide backbone amides is possibly responsible for the induced Soret–Cotton effect. Because there is no detailed information about the relative geometry of the haem and peptide, including the His side chains and helix axis orientations, we cannot exclude other possibilities for the origin of the Soret-CD bands, such as an asymmetrical axial ligation around the iron or the distortion (nonplanarity) of the haem plane upon binding to the peptides. However, the haem bound to the peptides was predominantly in its low-spin form, in which the axial ligands were identical His residues on the identical two α-helices. Therefore, the induced Soret-CD signal in our case probably does not arise from an asymmetrical axial ligation of the haem iron. Furthermore, it is also unlikely that the large distortion of the porphyrin ring was induced by the binding to the peptides, because high energy will be required to distort iron porphyrins.[45]

When the intensity of the Soret-CD band is compared among the haem–peptide complexes (Table 3), the haem bound to the peptides, except H2α(17)-L6, showed large and comparable values. On the other hand, H2α(17)-L6, which has six Leu residues per helix, showed only one third of the Soret intensity of the haem bound to the other peptides. These results suggested that the haem bound to the peptides H2α(17)-L4, H2α(17)-L4S, cH2α(17)-L4 and cH2α(17)-L4S, existed in more fixed orientation in the peptide 3D structure compared to

Table 3 CD spectral data of the haem bound to the peptides at the Soret band in the buffer and 15% TFE solution at 25 °C[a]

	$[\theta]_{max}/10^4$ deg cm^2 dmol^{-1} (λ_{max}/nm)		$[\theta]_{min}/10^4$ deg cm^2 dmol^{-1} (λ_{min}/nm)	
Peptide	Buffer	15% TFE	Buffer	15% TFE
H2α(17)-L6	7.74 (408)	4.28 (404)	−1.02 (391)	−0.69 (390)
H2α(17)-L4	21.8 (409)	6.63 (406)	−9.71 (393)	−1.35 (390)
cH2α(17)-L4	19.8 (408)	13.1 (406)	−8.84 (393)	−4.42 (391)
H2α(17)-L4S	17.9 (406)	7.99 (405)	−6.83 (390)	−1.28 (389)
cH2α(17)-L4S	19.3 (407)	13.1 (405)	−8.31 (390)	−3.55 (392)

[a] [haem] = 1.0×10^{-5} mol dm^{-3}, [peptide] = 1.2×10^{-5} mol dm^{-3}.

H2α(17)-L6. The orientation of the haem bound to the peptides seemed to be determined by the amino acid composition around the haem binding site, because there was a significant difference in the sequence between H2α(17)-L6 and other peptides in the arrangement and number of Leu residues. Generally, when the haem is bound to an apoprotein, such as apomyoglobin, in different orientations, the haem shows a weaker CD intensity relative to that when the haem exists in the "correct" conformation. For example, in natural haemproteins, a time-dependent increase in the Soret-CD band following reconstitution of haem to apoproteins has been reported and this is also considered as evidence for the haem reorientation between two interconvertable haem configurations.[46] In our case, the haem bound to H2α(17)-L6 might take several orientations in the peptide structure, because H2α(17)-L6 had a large hydrophobic face in its interior with six Leu residues per helix arranged around the haem-binding site. On the other hand, the hydrophobic area of the other peptides was composed of four Leu residues per helix with the same arrangement. The restricted interaction between the haem and the α-helices might require the haem to take fewer preferable orientations. The weaker intensity of the Cotton effect of the haem bound to H2α(17)-L6 relative to the other four peptides might be interpreted as the result of the haem taking various orientations. On the other hand, in our opinion, the haem bound to the peptides H2α(17)-L4, H2α(17)-L4S, cH2α(17)-L4 and cH2α(17)-L4S seemed to be fixed in the peptide structure with one major orientation.

In the buffer containing 15% TFE, the haem bound to the peptides also showed induced CD peaks similar to the spectra in the buffer. However, the intensity of the Soret-CD band of haem bound to the peptides in 15% TFE was only 1/2~2/3 of that in the buffer [Fig. 7(*b*) and Table 3]. Dissociation of the haem from the peptides cannot explain the reduced Soret-CD band, because the titration experiments indicated that the binding constants of the peptides to the haem were not significantly different from those in the buffer (Table 2). In the 15% TFE solution, it is expected that the hydrophobic interactions between the helices and the haem were weakened. Therefore, the haem could be free to take any orientation in the peptide structure and the number of the adaptable haem orientations in the binding site would increase. This would be responsible for the decrease in the intensity of the Soret-CD band in the 15% TFE solution relative to that in the buffer solution.

The CD features of haem bound to the coiled-coil type peptides H2α(14), H2α(17) and H2α(21), were also investigated in the 15% TFE–buffer solution. Interestingly, the haem bound to H2α(14), H2α(17) and H2α(21) in 15% TFE did not show a pronounced CD peak in the Soret band. These results also implied that these peptides bound the haem with more variable orientations than the other peptides. Because the orientation of the haem was not regulated in the peptide, the haem bound to H2α(14), H2α(17) and H2α(21) seemed not to show a significant Soret-CD band. The results of the Soret-CD studies demonstrated that the hydrophobic interaction between the haem and the peptide was important for the orientation of the haem, which could be regulated by the amino acid composition around the haem binding site.

Peroxidase-like activity of haem bound to the peptides

The diverse biological functions of haem seem to be determined by the axial ligands, 3D structure and the arrangements of amino acid residues surrounding the haem active site. In order for the haem to fulfill a specific function, natural proteins prevent other haem-functions. For example, natural electron-transfer proteins, cytochrome *b* or cytochrome *c*, contain haem characterized by His/His or His/Met bis-axial coordinations, respectively. The tight 6-coordination of haem prevents the direct reaction with an oxygen molecule or hydrogen peroxide which is characteristic of myoglobin or peroxidase, respectively, and therefore the proteins having only a physiological role in the electron transfer reaction. In our design of haem-conjugated peptides, haem was fixed in the polypeptide 3D structure by the bis-His coordinations, similar to natural *b*-type haemproteins. Thus, as the peptide binds the haem more tightly, the haem reacts less readily with a substrate, such as hydrogen peroxide. According to this assumption, we examined the catalytic activity of the haem bound to the peptides in 0.1 mol dm^{-3} Tris HCl buffer, pH 7.4, and in the 15% TFE–buffer solution using an oxidation reaction of *o*-methoxyphenol to its tetramer, tetraguaiacol, which is one of the typical reactions catalyzed by peroxidase or monooxygenase in the family of haemenzymes.[47] The determined initial rates are summarized in Fig. 8. In the buffer [Fig. 8(*a*)], the initial rate, *v*, of the reaction in the presence of peptide H2α(17)-L4S (0.76×10^{-6} mol dm^{-3} min^{-1}), was suppressed to a relative activity of 0.15 [relative activity, 1.0 in the absence of peptide (5.1×10^{-6} mol dm^{-3} min^{-1})]. The reaction rates of haem bound to peptides H2α(17)-L4, cH2α(17)-L4 and cH2α(17)-L4S, were also diminished to 0.77–0.96×10^{-6} mol dm^{-3} min^{-1}. These *o*-methoxyphenol oxidation activities were comparable to that of the natural electron transfer protein cytochrome *c* (0.32×10^{-6} mol dm^{-3} min^{-1}).[47] These results suggested that the haem was tightly fixed in the polypeptide 3D structure at a level similar to the natural bis-ligated haemproteins. In contrast, the reaction was weakly suppressed by the addition of H2α(17)-L6 (3.4×10^{-6} mol dm^{-3} min^{-1}, 0.66). The moderate suppression of haem reactivity by H2α(17)-L6 appeared to reflect a looser coordination by the axial ligands relative to the other peptides. As described above, the smaller K_a and weaker Soret-CD band intensity were attributed to the loosened coordination by the axial ligands in H2α(17)-L6. On the other hand, the peptides H2α(14), H2α(17) and H2α(21), which did not bind the haem in the buffer, did not influence the reaction rate of haem at all. These results confirmed that the suppression of catalytic reactivity by the addition of peptides was due to the formation of a peptide–haem complex in the solution.

In the 15% TFE solutions [Fig. 8(*b*)], the initial rate of reaction in the presence of the peptides H2α(17)-L4, H2α(17)-L4S, cH2α(17)-L4 and cH2α(17)-L4S, was also diminished to relative activities of 0.6–0.3. However, the suppression effects by the peptides in 15% TFE were weaker than those in the buffer. These results, in accordance with the CD results, suggested that the addition of TFE reduced the hydrophobic interaction between the haem and peptides, resulting in the haem reactivities in the peptides being slightly enhanced. On the other hand, the catalytic activities of haem bound to H2α(14), H2α(17) and H2α(21) in 15% TFE, were accelerated by factors of 2.0–2.6, relative to that in the absence of the peptides. These *o*-methoxyphenol oxidation activities of haem–peptide conjugates were comparable to that of bilayer-bound cytochrome *c* as reported by Hamachi *et al.*[47] These authors suggested that the activity of cytochrome *c* was generated by a small structural change around the haem, such as dissociation of the axial

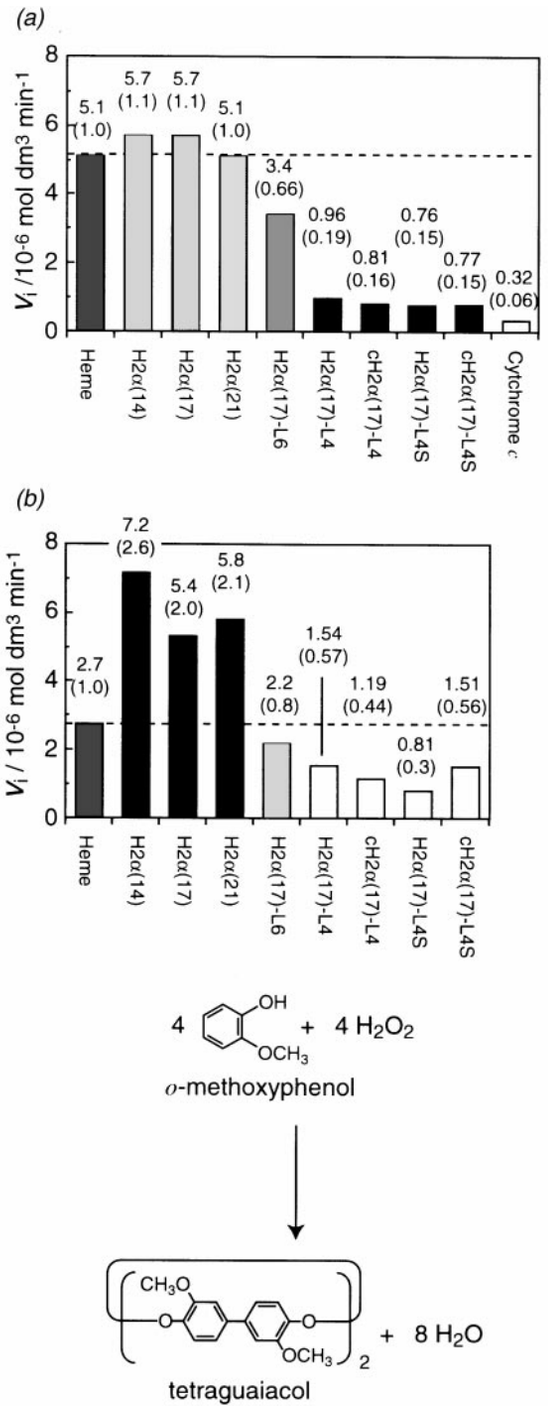

Fig. 8 Initial rates of tetraguaiacol formation catalyzed by the haem in the presence of peptides in (*a*) 0.1 mol dm^{-3} Tris HCl buffer, pH 7.4, and (*b*) 15% TFE–buffer solution at 25 °C. [haem] = 0.5×10^{-5} mol dm^{-3}, [peptide] = 1.0×10^{-5} mol dm^{-3}, [*o*-methoxyphenol] = 1.0×10^{-2} mol dm^{-3}, [H_2O_2] = 0.5×10^{-3} mol dm^{-3}.

ligand (Met^{80}), *via* the bilayer interaction of the protein. In our case, since the coordination of the axial His ligand in 15% TFE appeared to be weaker than that in the natural haemproteins, the haem bound to the peptides H2α(14), H2α(17) and H2α(21) allowed easier coordination of H_2O_2 to one side of the axial sites of haem and subsequent reaction at the haem center. It was suggested that the rate-determining step in our case was the formation of the active intermediate from the haem and H_2O_2, because the initial rate was dependent on the concentration of H_2O_2, but not on that of the substrate. Therefore, the peptide could enhance the activity by isolating the haem in the peptide structure from the haem-aggregates in solution, and form the active intermediate more easily. The catalytic activity accelerated by the disordered structure of cytochrome *c* or the 2α-helix peptides could be characterized as that of a catalytic molten globule suggested by DeGrado.[48] The results observed by using our designed peptides demonstrated that the catalytic activity of haem was correlated to binding and fixing abilities of the peptides observed by UV–VIS and CD studies (Fig. 9) and that the catalytic activity could be regulated by the simply designed polypeptide structures.

Discussion

It has been demonstrated that two series of 2α-helix peptides, which bound a haem cofactor through the ligation of two His residues, were successfully designed and synthesized. The first series of peptides, which were designed on the basis of the coiled-coil motif, showed a unique haem binding property which was dependent on TFE concentration. These peptides demonstrated some structural requirements for effective haem binding. For example, the peptides H2α(14) and H2α(17) bound the haem only when the 2α-helix structure was annealed by the addition of 10–25% TFE, indicating that the 2α-helix structure and consequent formation of hydrophobic pockets were essential for the haem binding. In addition, the construction of the 2α-helix structure and the presence of His at the hydrophobic face of two α-helices appeared to be insufficient to achieve the haem binding, because it was needed for the haem binding of the peptide H2α(21) to lose the tight helix–helix interaction by the addition of TFE. Although an excess amount of TFE caused a decrease of the binding constant due to the destruction of the peptide 3D structure and the loss of the hydrophobic interactions between the haem and peptides, the appropriate amount of TFE seemed to induce the structural refinement of the peptide and to assist the haem binding. These results showed that the peptide conformation, the rigidity of the helix–helix interaction at the haem binding site and the topology of the His residues were important for effective haem binding. The Soret-CD study of the haem bound to the peptides in 15% TFE suggested that the haem was randomly oriented in the binding site. This result also implied the structural insufficiency of the peptides for fixed haem binding.

In accordance with the above results, an amphiphilic α-helix, but not a coiled-coil, was used in the design of the second series of peptides, in which a His ligand was positioned at the center of the helix and in the hydrophobic region. In contrast to the first series of peptides, the peptides with the improved design took an α-helix structure in the buffer and bound the haem with higher affinities. The UV–VIS and CD properties of haem bound to the peptides indicated that the haem was predominantly in the low-spin state with two axial His ligands and was highly oriented in the haem binding pocket. However, among the second series of peptides, H2α(17)-L6 showed a lower affinity for haem and the intensity of the Soret-CD band for haem bound to L6 was smaller than other peptides, suggesting the haem binding state in H2α(17)-L6 was subtly flexible. A more successful design was achieved by H2α(17)-L4S, which showed a higher α-helix content, a larger binding constant and a stronger induced Soret-CD band. These results demonstrated that the number and arrangement of Leu residues forming the haem binding site in the 2α-helix structure were important in determining strong haem binding and fixing abilities to the peptide.

The difference in the binding and the fixing abilities for the haem by the peptides was significantly reflected by the peroxidase activity of haem. That is, the peptide possessing a stronger binding ability (larger K_a) and fixing ability (stronger Soret-CD peak) of the haem more effectively prevented the susceptibility to the oxidant, H_2O_2 (Fig. 9). Contrary to the expected properties for the *b*-type haem design, the first series of peptides accelerated the reactivity of the haem in the 15% TFE solution. These peptides bound the haem rather more

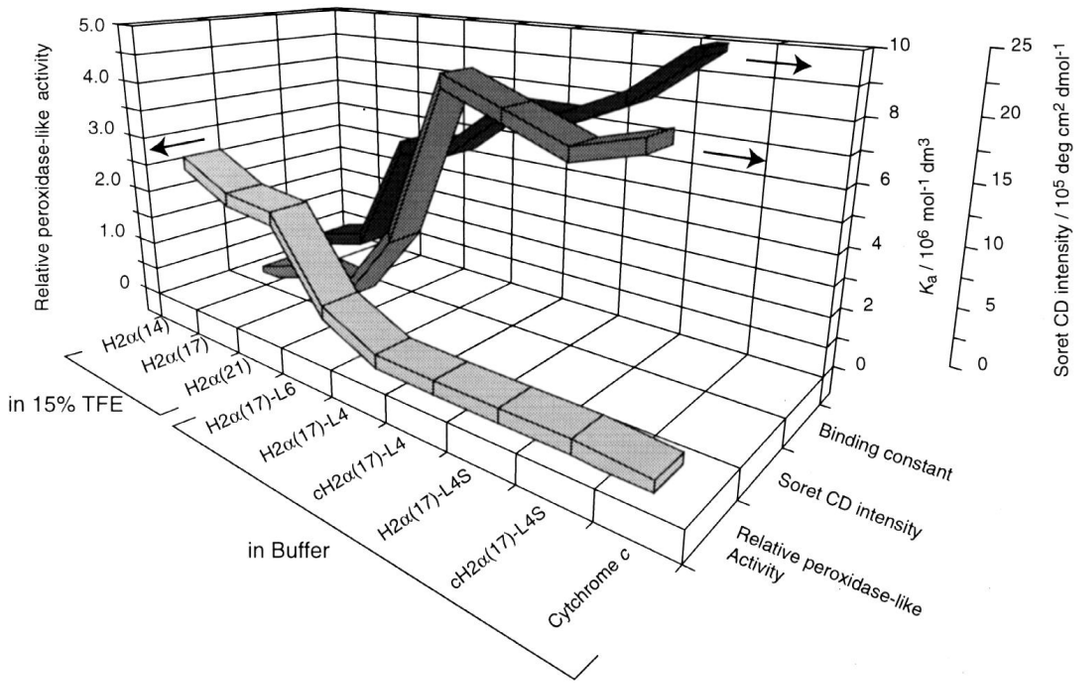

Fig. 9 Relationship between binding constants (black) of peptides for the haem, Soret-CD intensities (dark gray) and catalytic activities (light gray) of haem bound to the peptides.

loosely than the second series of peptides, which was suggested by the smaller K_a and no significant Soret-CD peak. The acceleration of haem reactivity might be due to this weaker interaction between the haem and peptides. On the other hand, except H2α(17)-L6, the second series of peptides significantly suppressed the haem catalytic activity. These peptides showed a larger K_a and a larger Soret-CD peak, suggesting that these peptides bound the haem more tightly than the others. Possibly, suppression of the catalytic reactivity of the haem–peptide conjugates was due to the tight packing of two α-helices with the haem. The tightness was accomplished by the arrangement of the His residue as a ligand and the hydrophobic Leu residues forming the haem binding site. Although detailed examination of the 3D structure of haem–peptide conjugates will be needed, further systematic substitution of amino acids forming the haem-binding site, including the axial ligands, will lead to the design of artificial haemproteins with a variety of specific functions with minimum structural elements.

Experimental

Peptide synthesis

The peptides were synthesized by the Fmoc solid-phase method according to the reported procedure[14b] using benzotriazol-1-yloxytris(dimethylamino)phosphonium hexafluorophosphate and 1-hydroxybenzotriazole hydrate as coupling reagents. H2α(14), H2α(17), H2α(21) and H2α(17)-L6 were synthesized using acetamidomethyl (Acm) as a protecting group for Cys at the C-terminal to obtain 1α-peptides. The Acm group in these peptides was removed according to the method of Yoshida *et al.*[49] H2α(17)-L4 and H2α(17)-L4S were synthesized using triphenylmethyl (Trt) as a protecting group of Cys at the C-terminal. The disulfide bond was formed by air-oxidation. cH2α(17)-L4 and cH2α(17)-L4S were synthesized using different sulfhydryl protecting groups to form intramolecular disulfide bonds selectively (Cys group at the N- and C-terminals were protected with the Acm and Trt groups, respectively). The disulfide bond at C-terminal in these peptides was formed by air-oxidation. The intramolecular second disulfide linkage at the N-terminal in cH2α(17)-L4 and cH2α(17)-L4S was formed using the silyl chloride–diphenylsulfoxide system reported by Akaji *et al.*[33] Peptides were purified with HPLC to give the products with a single peak on analytical HPLC using a linear gradient of acetonitrile–0.1% trifluoroacetic acid (TFA). Peptides were identified by MALDI-TOFMS and amino acid analysis; TOFMS; H2α(14), *m/z* 3529.6 $[(M + H)^+]$ (calcd. = 3529.1); H2α(17), *m/z* 4039.1 $[(M + H)^+]$ (calcd. = 4039.8); H2α(21), *m/z* 5036.9 $[(M + H)^+]$ (calcd. = 5036.9); H2α(17)-L6, *m/z* 4001.3 $[(M + Na)^+]$ (calcd. = 4001.8); H2α(17)-L4, *m/z* 4011.8 $[(M + H)^+]$ (calcd. = 4011.7); H2α(17)-L4S, *m/z* 4011.4 $[(M + H)^+]$ (calcd. = 4011.7); cH2α(17)-L4, *m/z* 4558.8 $[(M + H)^+]$ (calcd. = 4558.5); cH2α(17)-L4S, *m/z* 4558.3 $[(M + H)^+]$ (calcd. = 4558.5).

CD measurements

CD spectra were recorded on a Jasco J-600 or J-720 spectropolarimeter using a quartz cell with a 1.0 mm pathlength in the amide region (190–250 nm) and 10 mm in the Soret region (300–500 nm), respectively. H2α(14), H2α(17) and H2α(21) were dissolved in 2.0×10^{-2} mol dm^{-3} Tris HCl buffer (pH 7.4) containing various amounts of TFE in a peptide concentration of 2.0×10^{-5} mol dm^{-3}. H2α(17)-L6, H2α(17)-L4, H2α(17)-L4S, cH2α(17)-L4 and cH2α(17)-L4S were dissolved in the buffer in a peptide concentration of 1.0×10^{-5} mol dm^{-3}. Unfolding transitions were followed by plotting the ellipticity at 222 nm as a function of temperature (0–100 °C). The fraction of peptide in the folded state was calculated as the fraction of the molar residue ellipticity at each temperature relative to the initial molar ellipticity at 0 °C. The melting temperature, T_m, was then taken as the temperature at which half of the peptide was unfolded.

UV–VIS measurements

UV–VIS spectra were recorded on a SHIMADZU UV-3100 spectrophotometer using a quartz cell with a 10 mm pathlength. Mesoporphyrin IX was converted to the ferric complex by refluxing with excess $Fe(OAc)_2$ in acetic acid.[50] Iron mesoporphyrin in the buffer was titrated with peptides in increments of about 0.2 equiv. After each addition of peptide, samples were equilibrated for 30 min at 25 °C, then UV–VIS spectra (250–700

nm) were measured. The increase in absorbance at the Soret band with increasing peptide concentration was corrected for dilution and fitted by a single site binding equation[37] using Kaleida Graph (Synergy Software).

Assay for *o*-methoxyphenol oxidation

The *o*-methoxyphenol oxidation activity of haem in the presence or absence of the peptides was assayed by measuring the amount of the produced tetramer.[47] The reaction was initiated by the addition of hydrogen peroxidase (the final concentration, 0.5×10^{-3} mol dm^{-3}) to mixtures of *o*-methoxyphenol (substrate) (1.0×10^{-2} mol dm^{-3}), haem (5×10^{-6} mol dm^{-3}) and peptide (1.0×10^{-5} mol dm^{-3}) in 0.1 mol dm^{-3} Tris HCl buffer, pH 7.4, or 15% TFE–buffer, pH 7.4, at 25 °C. The reaction was followed by monitoring the absorbance change at 470 nm ($\varepsilon = 2.66 \times 10^4$ cm^{-1} M^{-1}).

Acknowledgements

We are grateful to Professor H. Aoyagi and Dr T. Niidome, Nagasaki University, for amino acid analyses.

References

1 *The Porphyrins*, ed. D. Dolphin, Academic Press, New York, 1979, vol. 7.
2 *Cytochrome P450*, *Structure*, *Mechanism and Biochemistry*, ed. P. R. Oritz de Montellano, Plenum Press, 1986.
3 S. A. Waldman, F. Murad, *Pharmacol. Rev.*, 1987, **39**, 163; M. A. Marletta, *J. Biol. Chem.*, 1993, **268**, 12231.
4 T. L. Poulous, *Adv. Inorg. Biochem.*, 1988, **7**, 2.
5 M. Momenteau and C. A. Reed, *Chem. Rev.*, 1994, **94**, 659.
6 B. Meunier, *Chem. Rev.*, 1992, **92**, 1411.
7 J. P. Collman, X. Zhang, V. J. Lee, E. S. Uffelman and J. I. Brauman, *Science*, 1992, **261**, 1404.
8 R. Breslow, X. Zhang and Y. Huang, *J. Am. Chem. Soc.*, 1997, **119**, 4535.
9 S. F. Betz, D. P. Raleigh and W. F. DeGrado, *Curr. Opin. Struct. Biol.*, 1993, **3**, 601; J. W. Brison, S. F. Betz, H. S. Lu, D. J. Suich, H. X. Zhou, K. T. O'Neil and W. F. DeGrado, *Science*, 1995, **270**, 935.
10 M. Mutter and S. Vuilleumier, *Angew. Chem.*, *Int. Ed. Engl.*, 1989, **28**, 535.
11 K. W. Hahn, W. A. Klis and J. M. Stewart, *Science*, 1990, **248**, 1544.
12 M. Montal, M. S. Montal and J. M. Tomich, *Proc. Natl. Acad. Sci. USA*, 1990, **87**, 6929.
13 H. Morii, S. Honda, K. Ichimura and H. Uedaira, *Bull. Chem. Soc. Jpn.*, 1991, **64**, 396.
14 (*a*) H. Mihara, Y. Tanaka, T. Fujimoto and N. Nishino, *J. Chem. Soc.*, *Perkin Trans. 2*, 1995, 1133; (*b*) S. Sakamoto, H. Aoyagi, N. Nakashima and H. Mihara, *J. Chem. Soc.*, *Perkin Trans. 2*, 1996, 2319.
15 M. Lieberman, M. Tabet and T. Sasaki, *J. Am. Chem. Soc.*, 1994, **116**, 5035.
16 M. R. Ghadiri and M. A. Case, *Angew. Chem.*, *Int. Ed. Engl.*, 1993, **32**, 1594.
17 (*a*) L Baltzer, A.-C. Lundh, K. Broo, S. Olofsson and P. Ahlberg, *J. Chem. Soc.*, *Perkin Trans. 2*, 1996, 1671; (*b*) K. S. Broo, L. Brive, P. Ahlberg and L Baltzer, *J. Am. Chem. Soc.*, 1997, **119**, 11362; (*c*) K. S. Broo, L. Brive, R. S. Sott and L. Baltzer, *Folding Des.*, 1998, **3**, 303.
18 M. R. Ghadiri, J. R. Granja and L. K. Buehler, *Nature*, 1994, **369**, 301.
19 (*a*) C. T. Choma, J. D. Lear, M. J. Nelson, P. L. Dutton, D. E. Robertson and W. F. DeGrado, *J. Am. Chem. Soc.*, 1994, **116**, 856; (*b*) D. E. Robertson, R. S. Farid, C. C. Moser, J. L. Urbauer, S. E. Mulholland, R. Pidikiti, J. D. Lear, A. J. Wand, W. F. DeGrado and P. L. Dutton, *Nature*, 1994, **368**, 425; (*c*) F. Rabanal, W. F. DeGrado and P. L. Dutton, *J. Am. Chem. Soc.*, 1996, **118**, 473; (*d*) W. A. Kalbeck, D. E. Robertson, R. K. Pandey, K. M. Smith, P. L. Dutton and D. F. Bocian, *Biochemistry*, 1996, **35**, 3429; (*e*) F. Rabanal, B. R. Gibney, W. F. DeGrado, C. C. Moser and P. L. Dutton, *Inorg. Chim. Acta*, 1996, **243**, 213; (*f*) B. R. Gibney, S. E. Mulholland, F. Rabanal and P. L. Dutton, *Proc. Natl. Acad. Sci. USA*, 1996, **93**, 15041.
20 H. Morii, M. Ishimura, S. Honda and H. Uedaira, in *Peptide Chemistry 1995*, ed. N. Nishi, Protein Research Foundation, Osaka, 1996, p. 481.
21 H. K. Rau and W. Haehnel, *J. Am. Chem. Soc.*, 1998, **120**, 468.
22 R. A. Arnold, W. R. Sfelton and D. R. Benson, *J. Am. Chem. Soc.*, 1997, **119**, 3181.
23 (*a*) S. Sakamoto, S. Sakurai, A. Ueno and H. Mihara, *Chem. Commun.*, 1997, 1221; (*b*) S. Sakamoto, A. Ueno and H. Mihara, *Chem. Commun.*, 1998, 1073.
24 T. Sasaki and E. T. Kaiser, *J. Am. Chem. Soc.*, 1989, **111**, 380.
25 K. S. Akerfeldt, R. M. Kim, D. Gamac, J. T. Groves, J. D. Lear and W. F. DeGrado, *J. Am. Chem. Soc.*, 1992, **114**, 9656.
26 H. Mihara, N. Nishino, R. Hasegawa and T. Fujimoto, *Chem. Lett.*, 1992, 1805; H. Mihara, Y. Haruta, S. Sakamoto, N. Nishino and H. Aoyagi, *Chem. Lett.*, 1996, 1; H. Mihara, K. Tomizaki, T. Fujimoto, S. Sakamoto, H. Aoyagi and N. Nishino, *Chem. Lett.*, 1996, 187.
27 F. Nastri, A. Lombardi, G. Morelli, O. Maglio, G. D'Auria, C. Pedone and V. Pavone, *Chem. Eur. J.*, 1997, **3**, 340; G. D'Auria, O. Maglio, F. Nastri, A. Lombardi, M. Mazzeo, G. Morelli, L. Paolillo, C. Pedone and V. Pavone, *Chem. Eur. J.*, 1997, **3**, 350.
28 (*a*) D. R. Benson, B. R. Hart, X. Zhu and M. B. Doughty, *J. Am. Chem. Soc.*, 1995, **117**, 8502; (*b*) P. A. Arnold, D. R. Benson, D. J. Brink, M. P. Hendrich, G. S. Jas, M. L. Kennedy, D. T. Petasis and M. Wang, *Inorg. Chem.*, 1997, **36**, 5306; (*c*) M. Wang, M. L. Kennedy, B. R. Hart and D. R. Benson, *Chem. Commun.*, 1997, 883; (*d*) D. A. Williamson and D. R. Benson, *Chem. Commun.*, 1998, 961.
29 (*a*) W. D. Kohn, C. M. Kay, B. D. Sykes and R. S. Hodges, *J. Am. Chem. Soc.*, 1998, **120**, 1124; (*b*) E. K. O'Shea, J. D. Kelmm, P. S. Kim and T. Alber, *Science*, 1991, **254**, 539.
30 S. Marqusee and R. L. Baldwin. *Proc. Natl. Acad. Sci. USA*, 1987, **84**, 8898.
31 S. Futaki and K. Kitagawa, *Tetrahedron*, 1997, **53**, 7479.
32 E. Atherton and R. C. Sheppard, *Solid Phase Peptide Synthesis: A Practical Approach*, IRL Press, Oxford, England, 1989.
33 K. Akaji, T. Tatsumi, M. Yoshida, T. Kimura, Y. Fujiwara and Y. Kiso, *J. Am. Chem. Soc.*, 1992, **114**, 4137.
34 J. M. Scholtz and R. L. Baldwin, *Annu. Rev. Biophys. Biomol. Struct.*, 1992, **21**, 95.
35 J. M. Scholtz, H. Qian, E. J. York, J. M. Stewart and R. L. Baldwin, *Biopolymers*, 1991, **31**, 1463.
36 C. Transford, *Adv. Protein Chem.*, 1962, **17**, 69.
37 T. Kuwaraba, A. Nakamura, A. Ueno and F. Toda, *J. Phys. Chem.*, 1994, **98**, 6297.
38 *The Porphyrins*, ed. D. Dolphin, Academic Press, New York, 1979, vol. 3.
39 M. S. Hargrove and J. S. Olson, *Biochemistry*, 1996, **35**, 11310.
40 W. R. Fisher, H. Taniushi and C. J. Anfinsen, *J. Biol. Chem.*, 1973, **248**, 3188.
41 E. M. Storch and V. Daggeet, *Biochemistry*, 1996, **35**, 11596; C. D. Moore and J. T. Lecomte, *Biochemistry*, 1990, **29**, 1984; C. D. Moore, O. N. Al-Misky and J. T. Lecomte, *Biochemistry*, 1991, **30**, 8357.
42 Y. Feng and S. G. Sliger, *Biochemistry*, 1991, **30**, 10150.
43 M.-C. Hsu and R. W. Woody, *J. Am. Chem. Soc.*, 1971, **93**, 3515.
44 T. Mizutani, T. Ema, T. Yoshida, T. Renne and H. Ogoshi, *Inorg. Chem.*, 1994, **33**, 3558.
45 J. D. Hobbs and J. A. Shelnutt, *J. Protein Chem.*, 1995, **14**, 19.
46 R. Santucci, F. Ascoli, G. N. La Mar, R. K. Pandey and K. M. Smith, *Biochem. Biophys. Acta*, 1993, **1164**, 133; R. Santucci, J. Mintrovitch, I. Constantinidis, J. D. Satterlee and F. Ascoli, *Biochem. Biophys. Acta*, 1988, **953**, 201; R. W. Right, R. J. Rohlfs, G. Palmer and J. S. Olson, *J. Biol. Chem.*, 1987, **262**, 46; A. Bellelli, R. Foon, F. Ascoli and M. Brunori, *Biochem. J.*, 1987, **246**, 787; H. S. Aojula, M. T. Wilson and A. Drake, *Biochem. J.*, 1986, **237**, 613.
47 A. Fujita, H. Senzu, T. Kunitake and I. Hamachi, *Chem. Lett.*, 1994, 1219.
48 W. F. DeGrado, *Nature*, 1993, **365**, 488; K. Johnsson, R. K. Allemann, H. Widmer and S. A. Benner, *Nature*, 1993, **365**, 530; H. Mihara, K. Tomizaki, N. Nishino and T. Fujimoto, *Chem. Lett.*, 1993, 1533; K. S. Broo, H. Nilsson, J. Nilsson, A. Flodberg and L. Baltzer, *J. Am. Chem. Soc.*, 1998, **120**, 4063.
49 M. Yoshida, T. Tatsumi, Y. Fujiwara, S. Iinuma, T. Kimura, K. Akaji and Y. Kiso, *Chem. Pharm. Bull.*, 1990, **38**, 1551.
50 *Porphyrins and Metalloporphyrins*, ed. K. M. Smith, Elsevier, Amsterdam, 1975, p. 801.

Paper 8/05669B